BURSTING, BEATING, AND CHAOS IN AN EXCITABLE MEMBRANE MODEL

TERESA REE CHAY* AND JOHN RINZEL‡
*Department of Biological Sciences, University of Pittsburgh, Pittsburgh, Pennsylvania; and
‡Mathematical Research Branch, National Institute of Arthritis, Diabetes, Digestive and Kidney Diseases, National Institutes of Health, Bethesda, Maryland 20205

ABSTRACT We have studied periodic as well as aperiodic behavior in the self-sustained oscillations exhibited by the Hodgkin-Huxley type model of Chay, T. R., and J. Keizer (*Biophys. J.*, 1983, 42:181–190) for the pancreatic β-cell. Numerical solutions reveal a variety of patterns as the glucose-dependent parameter k_{Ca} is varied. These include regimes of periodic beating (continuous spiking) and bursting modes and, in the transition between these modes, aperiodic responses. Such aperiodic behavior for a nonrandom system has been called deterministic chaos and is characterized by distinguishing features found in previous studies of chaos in nonbiophysical systems and here identified for an (endogenously active) excitable membrane model. To parallel the successful analysis of chaos in other physical/chemical contexts we introduce a simplified, but quantitative, one-variable, discrete-time representation of the dynamics. It describes the evolution of intracellular calcium (which activates a potassium conductance) from one spike upstroke to the next and exhibits the various modes of behavior.

INTRODUCTION

A wide variety of oscillation patterns have been observed in membrane potential recordings from β-cells of isolated pancreatic islets. Atwater et al. (1) found that as glucose conentration is increased the response evolves from a steady state of polarization into a bursting pattern with interburst period on the order of seconds. As glucose is increased adequately the bursting gives way to continuous spiking or beating. At very high glucose concentrations one finds a steady depolarization. These features are also found in the theoretical model of Chay and Keizer (2), a model of the Hodgkin-Huxley (3) type in which the depolarizing current is due to calcium rather than sodium ions.

Here, we examine in greater detail the transition between the beating and bursting modes for this theoretical model. We have found that for certain parameter ranges the transition regime is characterized by aperiodic responses—irregular bursting or irregular spiking. We emphasize that the model is deterministic so that this irregularity in the response cannot be explained in terms of any stochastic feature of the biophysical formulation. Rather, it reflects a not uncommon phenomenon in nonlinear dynamical systems often referred to as deterministic chaos.

Aperiodic dynamics and the transition from periodic to aperiodic behavior in other contexts has been studied ambitiously in recent years by chemists, physicists, and mathematicians. Some applications include the transition to turbulence in fluid dynamics (4), sustained oscillations in open chemical systems (5, 6), dynamics of nonlinear electronic circuits (7), and models of population dynamics in ecology (8). The literature in this area is vast; some recent reviews are (9–12). Experiments and theory have identified some distinguishing routes to chaos, i.e., characteristic sequences of successively more complex patterns as a parameter is adjusted. For example, one may observe a predictable heirarchy of doublet patterns (period-doubling cascade) as in (6, 8, 11). Another possibility is intermittency (13) in which long periods of relative regularity are abruptly and irregularly interrupted by bursts of quite different activity; the mean duration of regular periods grows predictably as a critical parameter value is approached. A useful quantitative tool for studying such chaotic behavior is a discrete time one-variable representation of the observed dynamics (e.g., see reference 5–8, 10–20).

Aperiodic responses have been observed both theoretically and experimentally for excitable cells driven by a sinusoidal stimulating current (14–16, 26). Period-multupling of the cardiac rhythm under drug application has been reported (18). Yet we know of no previous systematic identification of chaos in a model for a nondriven (endogenous) electrically excitable membrane system. Here we report that the Chay-Keizer model exhibits aperiodic responses as the parameter k_{Ca} (the rate of intracellular Ca^{++} uptake) is varied; decreasing this parameter in the model represents decreasing the glucose concentration. We find as k_{Ca} is decreased that loss of the regular beating mode is accompanied by a sequence of period-doublings which is succeeded by chaotic spiking. As k_{Ca} is decreased further we find that bursts of spikes begin to form.

However, these bursting patterns are aperiodic until k_{Ca} decreases adequately. We have supported and complemented these findings by a description of the dynamics in terms of a one-variable, discrete-time model that relates the level of intracellular calcium from one spike upstroke to the next. This map and its solution behavior correlate well with the full five-variable Chay-Keizer model. Although we present quantitative results, our analysis and interpretations are qualitative and we expect that the mechanism for aperiodic behavior which we have found may be operative in other excitable system.

THE MODEL AND ITS DYNAMIC BEHAVIOR

The β-cell model of Chay and Keizer (2) consists of five first-order, simultaneous, nonlinear equations containing the following dynamic variables: (*a*) n, the degree of activation for the voltage-dependent K^+-channel; (*b*) m, the degree of activation for the voltage-dependent Ca^{++}-channel; (*c*) h, the inactivation for the same channel; (*d*) the intracellular calcium concentration, denoted by Ca, whose rate equation consists of the inward calcium current and a first-order disappearance of Ca, written as k_{Ca} [Ca], where k_{Ca} is the rate constant; and (*e*) the membrane potential, V, whose time derivative is proportional to the sum of ionic currents carried by Ca^{++} and K^+ ions.

The differential equations representing these five dynamic variables were solved numerically on a DEC-10 computer (Digital Equipment Corp., Marlboro, MA) with a Gear algorithm, with absolute and relative error tolerances set at 10^{-7}. The parametric values used for our computations were taken from Table 1 of Chay and Keizer (2) with the exception of temperature that is taken here to be 17°C.[1] At this temperature, the plateau membrane potential of the active phase (i.e., spiking phase) becomes very close to the minimum repolarizing membrane potential of the silent phase. Period doublings and chaos shown below occur in the parameter region where the bursting mode becomes the beating mode.

Fig. 1 shows an overall view of the bursting-spiking patterns of the Chay-Keizer model as k_{Ca} is increased from 0.038 to 0.045 ms^{-1}. The left column of plots shows the time course of membrane potential and the right column that of intracellular calcium concentration. The uppermost panels (for k_{Ca} = 0.038 ms^{-1}) exhibit a periodic bursting pattern with the following qualitative features. The spikes appear to ride on a plateau potential and the interspike interval increases dramatically near the end of the burst. With each spike there is a net increase in calcium concentration and thereby further activation of the Ca-dependent potassium conductance. This rising conductance eventually inhibits the spiking mechanism and leads to the K^+-dominated silent phase. During the silent phase, calcium concentration decreases (through uptake mechanisms) and a slow depolarization develops. When the membrane potential reaches threshold for spike initiation the active phase is rekindled. The computed burst pattern and this description closely resemble those for experimentally observed β-cell responses in the presence of glucose. A noticeable quantitative difference is that for the temperature chosen here the burst has relatively few pulses (compare to Fig. 1 in reference 2).

The lowermost panels in Fig. 1 correspond to sufficient glucose (k_{Ca} = 0.045 ms^{-1}) to cause continuous spiking or beating. In this case there is zero net increment of calcium from one spike to the next; k_{Ca} is large enough so that calcium uptake by intracellular compartments during the interspike phase just balances the influx from membrane calcium current during the spike's depolarized phase. The two intermediate values of k_{Ca} result in aperiodic responses; even for much longer simulation times than shown in Fig. 1, we find no apparent periodicity. We refer descriptively to these two cases as chaotic bursting (k_{Ca} = 0.04 ms^{-1}) and chaotic spiking (k_{Ca} = 0.0415 ms^{-1}). Such irregular behavior is not due to numerical artifact nor to extraordinary parameter settings.

To obtain additional insight into the model's responses it is useful to view calcium as a dynamic parameter that regulates the faster time scale spiking mechanism and induces switching between the active and silent phases. This is illustrated graphically in the leftmost panels of Fig. 2, where the (five-variable) response trajectory is projected onto the Ca-V plane. Motion here is clockwise. Consider first the upper set of panels; these correspond to the uppermost case of Fig. 1. The periodic burst appears as a closed curve (upper left) whose upper elongated loops are the spikes and whose lower flat portion represents the silent phase. The triple-branched, dashed curve results from a pseudo–steady-state analysis of the model. When Ca is treated as a parameter the remaining variables V, m, h, n form an excitable subsystem that exhibits three different steady state or rest potentials (dashed curves in left panels) when k_{Ca} lies between the approximate values 0.315 and 1.884 μM. With calcium fixed (in this range) the lower steady potential is stable for the subsystem and the intermediate steady state has a saddle point structure with its associated threshold separatrix (21). The upper steady state in this example is not stable, as one might conjecture, but rather unstable. Moreover, for a subinterval of Ca values ($0.321 \geq Ca \geq -0.713$) it is surrounded (a vague but intuitive notion for the four-variable subsystem) by a stable Ca-dependent oscillation that corresponds to the repetitive spiking of the active phase. The minimum potential of this oscillation is relatively independent of Ca and this corresponds to the plateau potential of the active phase. Note, in this model, the upper steady state does not represent the plateau potential as it does in Plant's (22) treatment of the R-15 bursting pacemaker of *Aplysia*.

Now let us reconsider the burst pattern generated with Ca as a dynamic variable. As Ca increases from one spike

[1]Here the temperature 17°C corresponds to $3^{1.07}$.

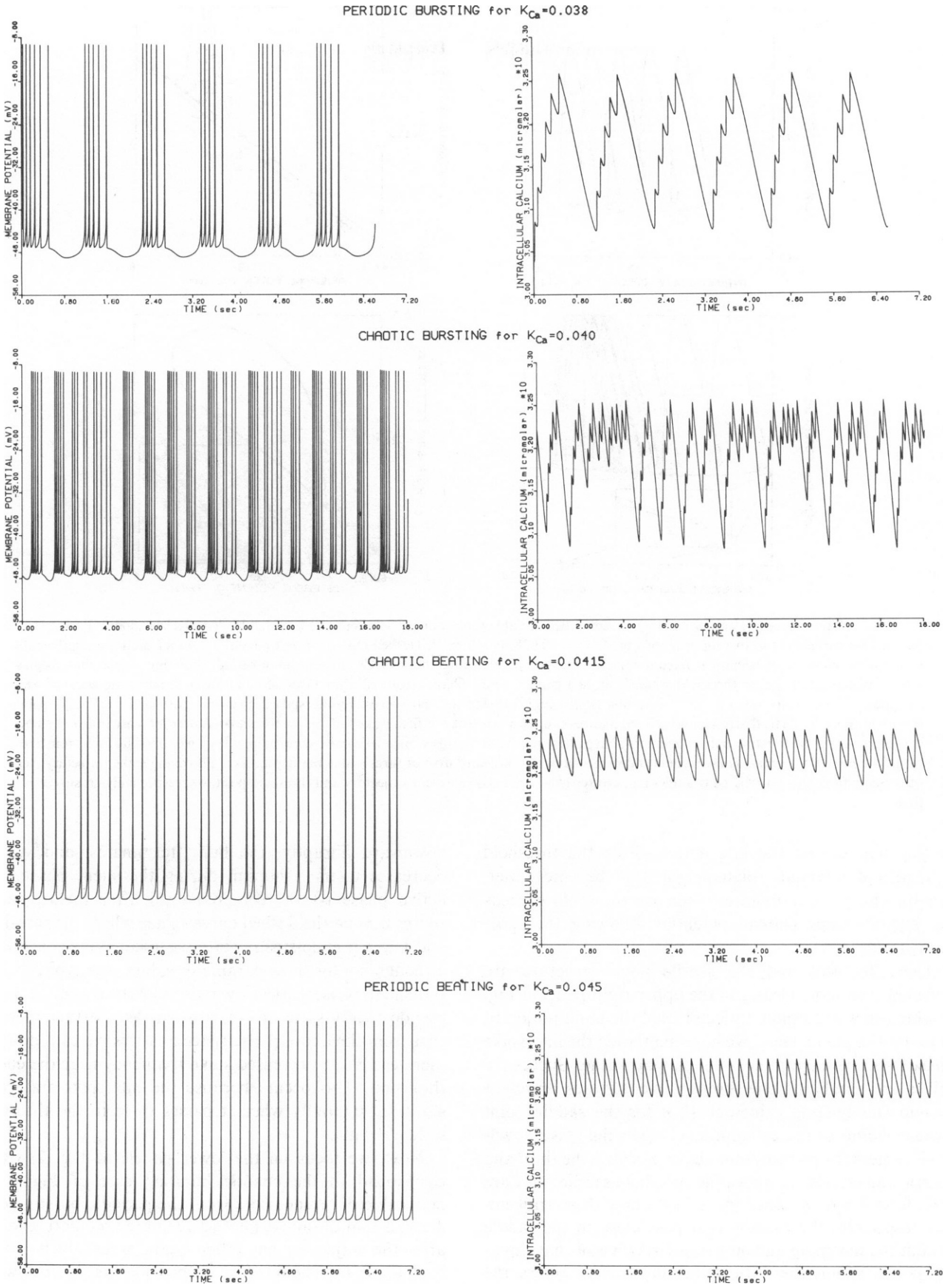

FIGURE 1 Various periodic and aperiodic responses of Chay-Keizer model and dependence upon k_{C_a} the (glucose-dependent) uptake rate of intracellular calcium. From *top* to *bottom* k_{C_a} = 0.038, 0.040, 0.0415, 0.045 ms^{-1}. *Left* column shows membrane potential vs. time; *right* column displays calcium concentration vs. time. Voltage and concentration scales are identical in all panels. Second row of panels has longer time duration (18 s) than others (7.2 s) to illustrate lack of periodicity in burst activity. Note that range of calcium variation in beating cases is much less than in bursting cases.

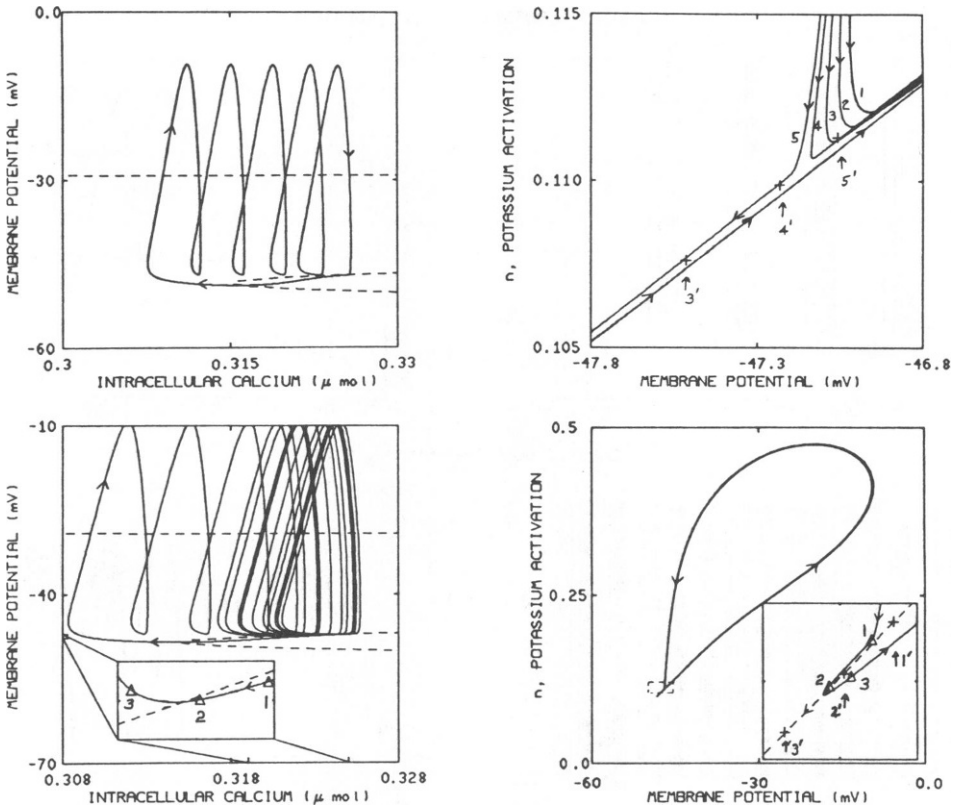

FIGURE 2 Phase space analysis of bursting based on two-variable projections of solutions to five-variable Chay-Keizer model. Two rows of panels here correspond to two top rows of Fig. 1: k_{Ca} = 0.038, 0.040 ms^{-1}. Dashed curves (in *left* panels) represent multiple steady-state potentials of model with calcium as fixed parameter. *Upper left* case shows the V vs. Ca closed orbit of periodic bursting. Silent phase begins when trajectory falls below threshold (*middle* dashed curve); active phase reentered after threshold and lower steady state coalesce and disappear. The corresponding n vs. V projection (*upper right*) illustrates that successive interspike trajectories pass closer to saddle point threshold (crosses, vertical arrows, and primed numbers) until downstroke of fifth spike falls below threshold. *Lower left* case illustrates how trajectory of chaotic bursting pattern reenters active phase prematurely (inset magnifies one example; inset region defined by lines from axes tics). The n vs. V projection (*lower right*) shows mechanism: downward drift of threshold actually overtakes polarizing spike trajectory (see *inset* magnification). Numbered triangles and crosses (*lower* panels) represent trajectory and threshold positions, respectively, at successive times.

to the next during the late active phase the threshold voltage and interspike plateau potential become closer. Finally, the burst terminates when the threshold exceeds the instantaneous plateau potential following the spike downstroke.

These features and the saddle point structure are revealed even more clearly in the upper-right panel of Fig. 2, which shows the spike trajectories of the burst projected onto the V-n plane. Here, we have magnified the interspike phase when voltage is near its plateau value. Successive spikes are numbered one through five. Crosses represent pseudo–steady-state values of V, n for the saddle point corresponding to the calcium level when the spike downstroke enters the picture from above. Because the third and fourth trajectories are above the threshold saddle, they are each followed by another spike. Note how these trajectories (especially the fourth) that pass close to the saddle exhibit the incoming and outgoing directions of that singular point. When the fifth spike downstroke enters the picture it is below threshold so the trajectory sweeps downward abruptly, the burst terminates, and voltage decreases to its minimum during the silent phase. The active phase is not reentered until after the trajectory passes beyond the dashed curve's knee where the threshold and lower pseudo-steady state coalesce. We remark that, although not for these parameter values, one typically sees the silent phase trajectory more closely track the lower pseudo-steady state of polarization. We further mention that from the above phase space analysis we can interpret more easily the decreased spike frequency near the end of the burst. This occurs because the interspike trajectory slows substantially when it passes close to the threshold saddle point.

Next, we focus on the lower panels of Fig. 2, which correspond to the chaotic bursting case of Fig. 1. A noticeable difference here from the periodic bursting case above is that the active phase is reentered prematurely, i.e., after the trajectory has fallen below threshold it crosses back above threshold before Ca has decreased to below the dashed curve knee. An example of this premature reentry

is shown in the inset magnification. To understand this behavior we must examine more closely the dynamics of the Ca-dependent threshold migration and the subsystem trajectory following the spike down stroke. Again we exploit the *V-n* projection (lower-right panel) where the many spikes of the aperiodic burst become overlaid. The pointed tail at the lower left of this trajectory corresponds to the interspike phases of near threshold and plateau potential behavior. The inset magnification isolates one particular threshold crossing event; it corresponds to the inset of the left panel. The triangles represent time marks on the trajectory, whereas the crosses represent the positions of the saddle point determined by the calcium concentration at the corresponding times. At the first two times the trajectory is below threshold. However, the saddle point is migrating leftward faster than the *V-n*

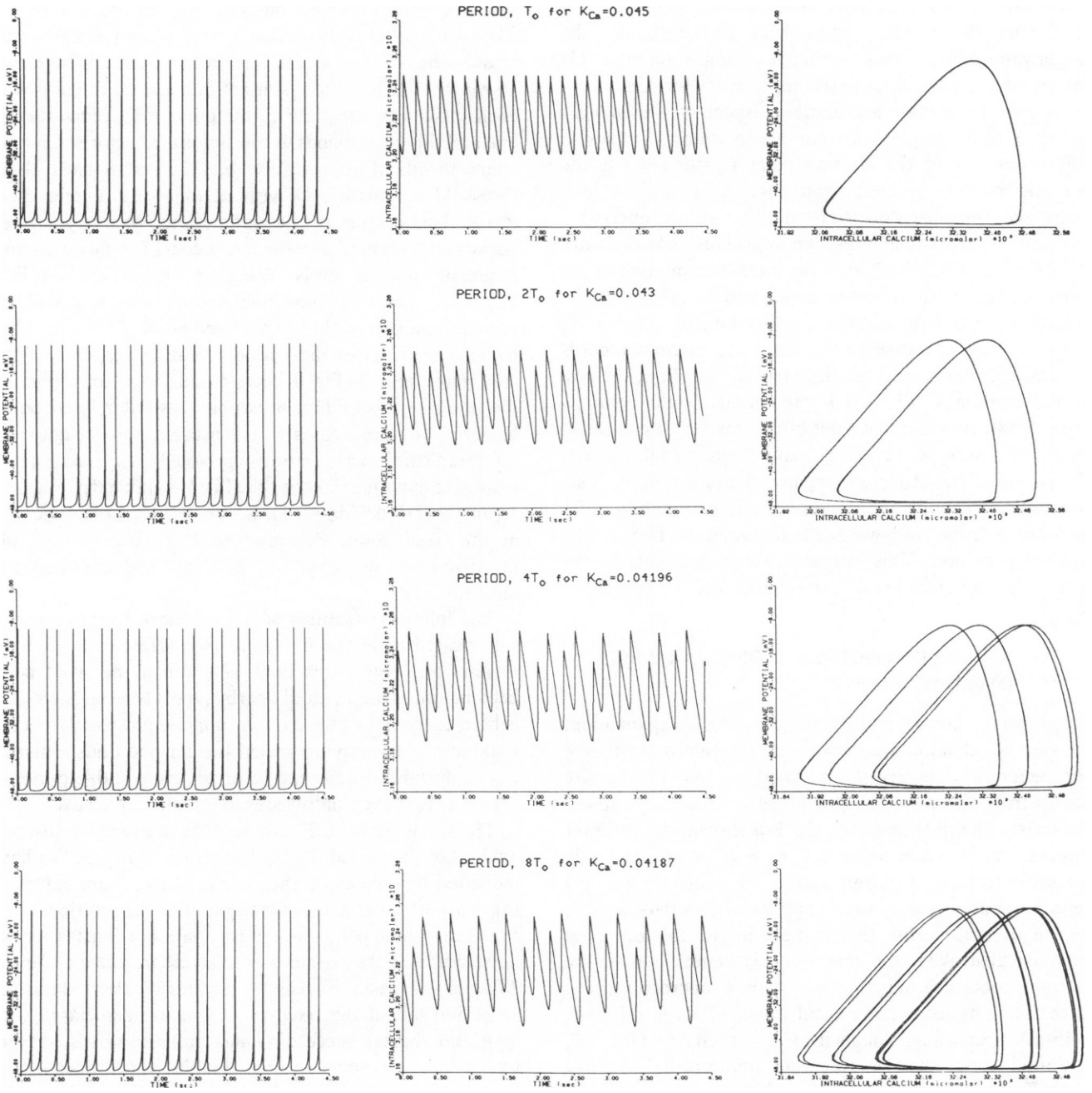

FIGURE 3 Sequence of period-doubling patterns as k_{Ca} is decreased from 0.045 ms^{-1} (the case of periodic beating). *Left* column: membrane potential vs. time; *middle* column: calcium concentration vs. time; *right* column: membrane potential vs. calcium concentration. Voltage time course shows spike doublets, whereas *middle* and *right* columns reveal greater detail of patterns. All panels in a given column have same scale.

trajectory and overtakes it before the third time mark. When this happens the V-n trajectory turns around, a spike upstroke is initiated, and the active phase is reentered prematurely. A major factor for this occurrence is the similar slow time scales of the voltage trajectory and the Ca-dependent saddle point migration. For parameter settings in which the repolarization of the silent phase is very rapid, the threshold has little opportunity to overtake the V-n trajectory and thereby cause premature reentry. Here, the repolarization is slow because the threshold and lower pseudo-steady state are very close together (so $|dV/dt|$ is small when the trajectory passes between them). Also, the larger value of k_{Ca} makes the threshold migration relatively faster, which contributes to the opportunity for reentry.

In Fig. 3 we illustrate another aspect of the model's behavior that complements our observations of chaos in this system. Here the starting point (upper row) is the periodic beating pattern from Fig. 1. As k_{Ca} is then decreased (proceed downward in Fig. 3), we observe a cascade of period doublings; the approximate periods are T_0, $2T_0$, $4T_0$, $8T_0$, where T_0 is the interspike interval of the basic beating pattern in the upper panels. Although the voltage time courses show little variation in the doublet patterns from one case to the next, the calcium records (middle column) reveal the fine structure of the successive period doublings. The Ca-V projections (right column) show vividly how a closed orbit bifurcates and is succeeded by a closed orbit with twice as many loops. At bifurcation, the period of the observed response doubles exactly. This bifurcation phenomenon is caused by loss of stability of a periodic solution and we shall discuss it further in the following section. This period-doubling cascade is evidently the route that leads to the chaotic beating pattern of Fig. 1.

APPROXIMATION BY A ONE-VARIABLE DYNAMIC MODEL

To motivate a one-variable dynamic model we again adopt the view of calcium concentration as a regulating dynamic parameter. We observe that throughout the active phase the upstroke-downstroke segments of the successive spikes are nearly identical (e.g., see the V-n trajectories in lower right of Fig. 2). Thus, because V, m, h, n follow essentially the same trajectory during each spike upstroke we may describe approximately the dynamics of this five-variable system by considering the changes in the calcium level from one upstroke to the next. For this we let C denote the calcium concentration at the -45-mV upcrossing of a spike. Then by using the typical values of m, h, n for the -45-mV upcrossing, along with $V = -45$ mV and Ca $= C$, as initial conditions we integrate numerically the five Chay-Keizer equations to obtain the calcium concentration $F(C)$ at the next -45-mV upcrossing. By considering a range of C values we thus generate the graph of $F(C)$. The evolution of C_n the calcium level at the nth spike upstroke to C_{n+1} is then described by the difference equation (or discrete map):

$$C_{n+1} = F(C_n). \tag{1}$$

We remark that although time is discrete in this formulation the implicit time increments are not equal because the interspike interval increases with Ca throughout the active phase. The approach we follow here is similar to that employed in (19, 20) to describe complex oscillation patterns of a chemical system.

In Fig. 4 we present the maps (shown dotted) corresponding to the four period-doubling examples of Fig. 3. They are qualitatively similar: a single-humped curve that crosses the 45° ray or 1:1 line exactly once. Where F is above the 1:1 line, there is a net increase of calcium with each spike. For adequate C_n the curve falls below the 1:1 line and this corresponds to continuous trajectories that fall below threshold after a spike but then cross back above threshold (prematurely) without following a long silent phase. This portion of the right branch of $F(C)$ is steep because the reentry phenomenon occurs for only a narrow range of calcium levels. Where F crosses the 1:1 line, $C_{n+1} = C_n$ and this fixed point corresponds to a discrete periodic solution of Eq 1. This fixed point of the upper left panel approximates the periodic beating response of the continuous model (Fig. 1 bottom and Fig. 3 top). Each of the other panels of Fig. 4 exhibits a similar fixed point, however, in those cases it is unstable and so does not represent stable periodic beating. Note that a fixed point of a discrete dynamical model like Eq. 1 is stable if $|dF/dC| < 1$ (unstable if $|dF/dC| > 1$), where dF/dC is the slope of F at the fixed point. Because this slope becomes steeply negative as k_{Ca} decreases in Fig. 4 the fixed point becomes unstable.

The following features of single-humped maps are now well described in the literature (see reference 8 and the reviews and references in 9–12). When the fixed point becomes unstable a pair of nearby points (one on each side) is born to form a stable 2 cycle (upper-right panel). As the parameter and map are varied further one finds a hierarchy of destabilizations and bifurcations to stable cycles of period 2^n that eventually leads to a regime of chaos.

The stable periodic 2^n-cycles of the map are the discrete analogs of the period-doubled solutions of Fig. 3. We have indicated by crosses on these maps the calcium values at the -45-mV upcrossings for the continuous solutions from Fig. 3 and these points fall on the map. For illustration we have indicated the presumptive discrete trajectories for the $2T_0$ and $4T_0$ cases. Successive iterates C_n alternate to the right and left of the fixed point and are associated with long and shorter succeeding interspike intervals, respectively; this corresponds to the doublet appearance of the continuous voltage records. We have also numerically iterated the map according to Eq. 1 and thereby verified convergence of the discrete solution to the corresponding discrete 2^0, 2^1, 2^2, and 2^3 cycles.

Next we interpret the patterns of Fig. 1 in terms of the

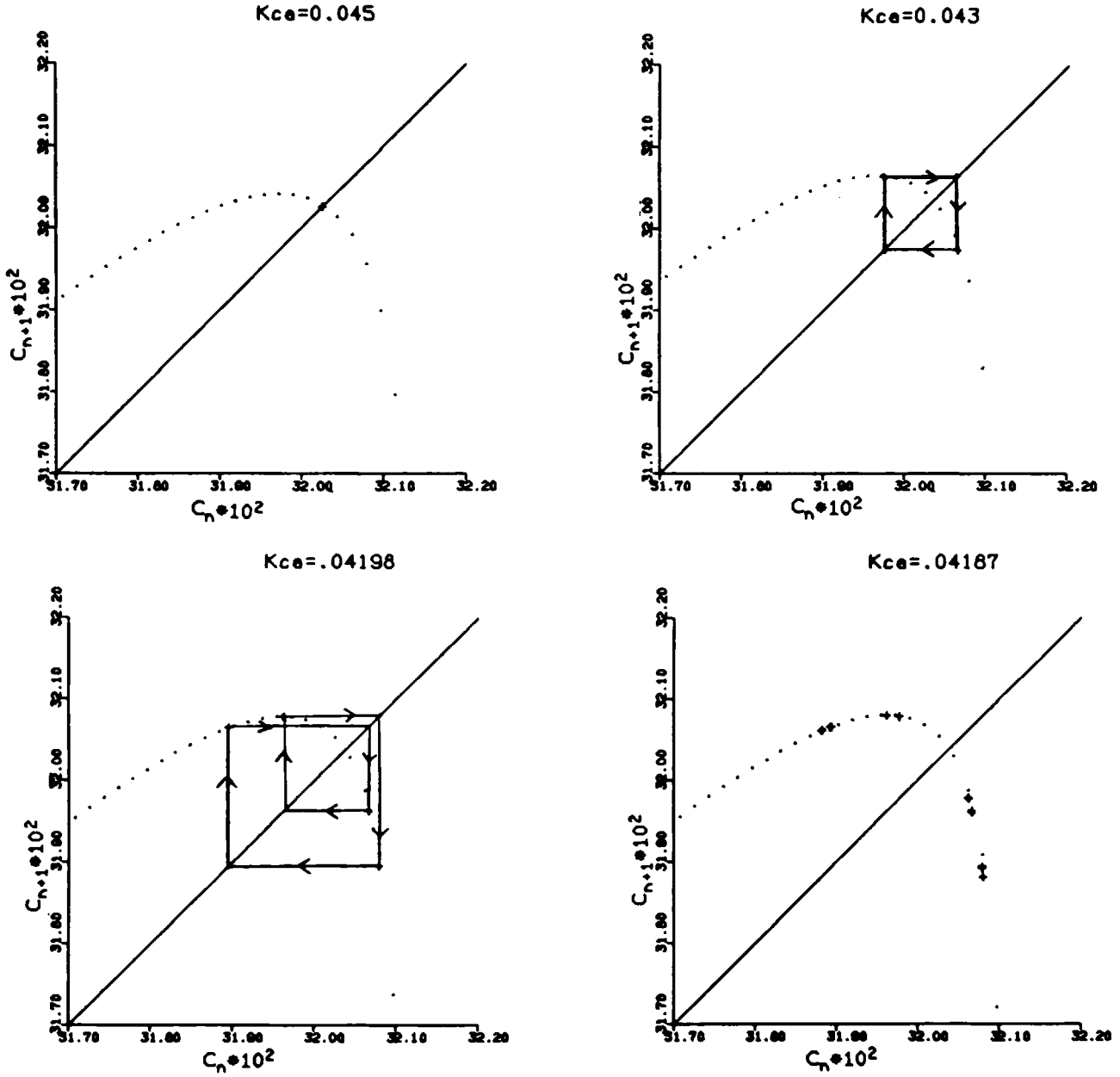

FIGURE 4 One-variable map representation (shown dotted) for discrete time dynamics of calcium concentration from one spike upstroke to the next (see description in text and Eq. 1). Four panels here correspond to period-doubling sequence of Fig. 3. Crosses represent calcium concentration at −45-mV upcrossing of continuous solution of Fig. 3. Fixed point of map (intersection with 45° line) corresponds to stable periodic beating in one case (k_{C_a} = 0.04 ms^{-1}); but in other cases fixed point is unstable and corresponds to unstable periodic solution of Chay-Keizer model.

map. For this the graph of F has been computed over a larger range of C values; computed maps are shown in Fig. 5 along with corresponding calcium data (shown as crosses) from the continuous solutions. Again the maps are qualitatively similar but now we clearly see evidence of the silent phase. For large enough C_n there is a large drop in calcium before the next upstroke. This reentry to the active phase occurs in a characteristic way after the voltage threshold and pseudo–steady-state potential of the silent phase have coalesced (see dashed curves of the Ca-V panels of Fig. 2). Moreover, this reentry point is relatively independent of the initial calcium level when it is high enough. Hence the map is flat for large C_n. As in Fig. 4, the steeply sloping right branch corresponds to premature reentry that occurs for any value of k_{C_a} but only for a narrow range of C_n values.

The effect of decreasing k_{C_a} is to increase the net increment of calcium from one spike to the next and thereby basically to move the map upward. This moves the fixed point onto the steep portion of the right branch; the

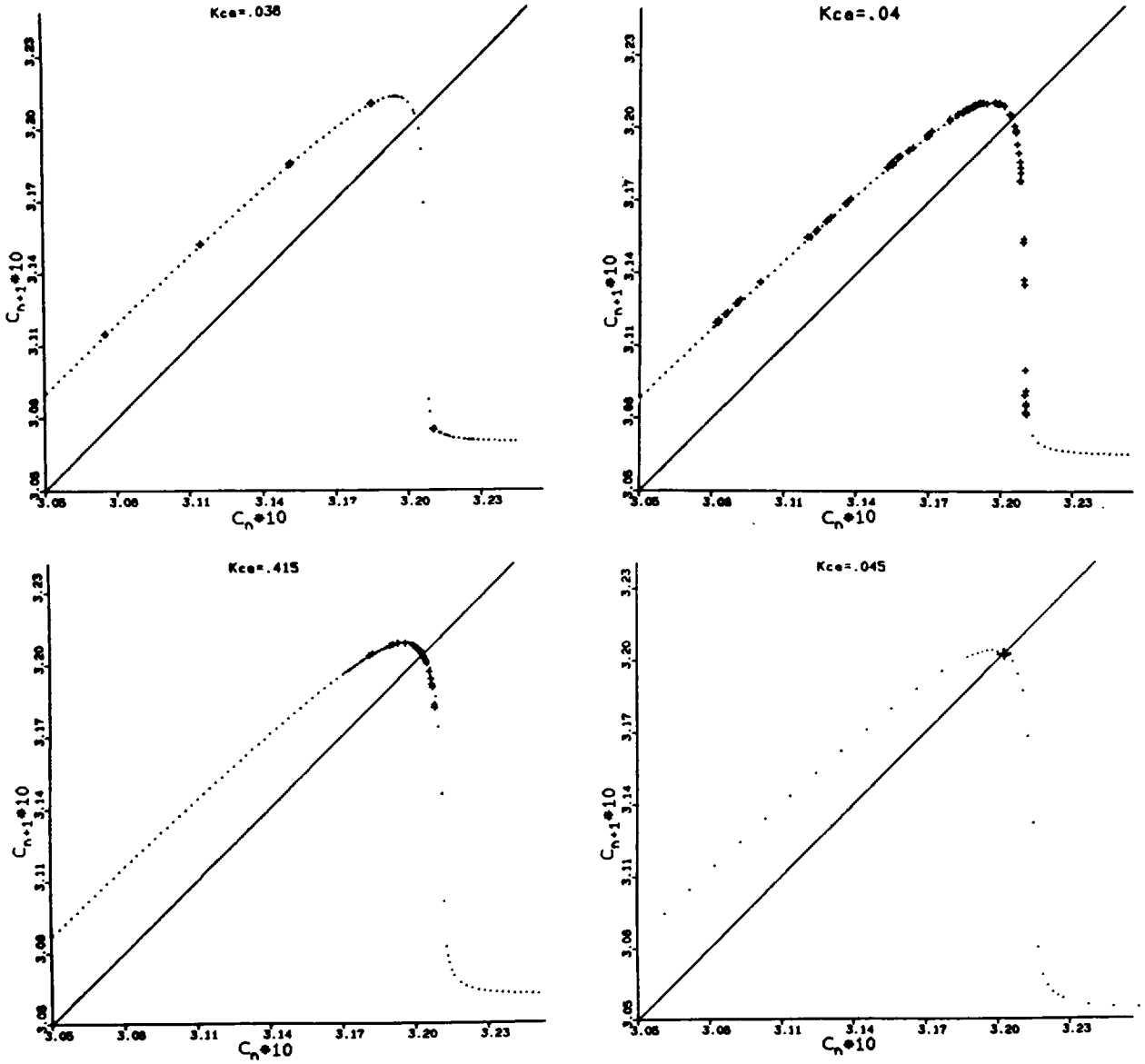

FIGURE 5 One-variable map representations (Eq. 1) for parameter values of Fig. 1. Crosses show calcium concentration at −45-mV upcrossing of continuous solutions of Fig. 1. For example, the case of periodic beating is represented by five points in upper *left* panel. The chaotic patterns nearly fill out subintervals over which the map is defined.

periodic beating pattern becomes unstable. To understand the chaotic patterns we notice carefully what action the map has on points near the relatively flat hump. Suppose such points are mapped onto the destabilizing steep right branch. Intuitively, any perturbation on such a C_n places a large uncertainty on the successor C_{n+1}. A periodic cycle containing such points is likely unstable. In the case of chaotic beating the hump is mapped only part way down the negative slope region and we see only fine-structured, locally contained chaos. For the case of $k_{Ca} = 0.04$ ms^{-1} however, points near the hump are mapped onto nearly the entire length of the destabilizing branch that in turn sends points over a large range of the left branch. Hence we observe premature reentry over a large range of calcium (lower left of Fig. 2) and the aperiodic response has a bursting appearance. Finally, for $k_{Ca} = 0.038$ ms^{-1}, the map ascends sufficiently for the hump to be mapped onto the lower flat portion and we observe the stable five-spike burst pattern. If k_{Ca} were decreased even further the left branch would move higher corresponding to greater net increment in calcium per spike. Hence fewer spikes would occur during the active phase. For $k_{Ca} = 0.035$ ms^{-1}, we find a periodic four-spike bursting pattern. There may, but not necessarily, be a narrow parameter range of fine-structured period-doubling and/or chaos between the five- and four-spike regimes.

DISCUSSION

We have examined some aspects of a model for excitable membrane electrical oscillations. We have shown that the

Chay-Keizer model for the pancreatic β-cell exhibits aperiodic responses in the parameter range for transition between the bursting and beating modes of activity. This dynamic behavior was illustrated numerically and analyzed via phase space concepts (threshold separatrices, multiple steady states, closed orbits, and reduced subsystems) and in terms of one-variable discrete maps. The success of these approaches rests on the biophysical motivation that calcium plays the influential role of a regulating dynamic parameter. This allows for a pseudo–steady-state analysis and also includes consideration of the subsystem's dynamics. For the discrete model, calcium is the only dynamic variable but the spike action potential and slow calcium uptake mechanisms are both accounted for in this description of the evolution of calcium level from one spike upstroke to the next.

The map representation is computed numerically here although, based on the phase space analysis, its general form could be qualitatively deduced. It allows a compact and simplified way to understand the beating and bursting modes and also the chaotic transition behavior. When k_{Ca} is high there is a smaller net increment in calcium from one spike to the next. This means the map's left branch is close to the 1:1 line and the fixed point is stable (Fig. 5, lower right). When k_{Ca} is low the net increment is greater (because of less uptake between spikes) and the map is higher. Then the fixed point corresponding to periodic beating is unstable and trajectories visit both the left branch and the lower flat right portion to develop a periodic bursting pattern (Fig. 5, upper left). For intermediate parameter values the map sends an interval of points near its maximum to the destabilizing steeply descending right branch and hence aperiodic behavior is observed.

The continuous model and map will maintain their qualitative features over a range of parameter variations so that one may expect aperiodic behavior elsewhere in parameter space. In some regimes, the parameter range for aperiodic activity may be very small or even nonexistent, for example, if transition behavior is dominated by hysteresis in which parameter intervals for different response patterns are overlapping (e.g., see reference 20). Here, we have adjusted the temperature to enhance the k_{Ca} range over which chaos is found. In this case, the spiking plateau potential is close to the silent phase minimum potential. We suggest that this may provide at least one observable signature by which to guide parameter selection for possible systematic experimental investigation of aperiodic phenomena in the transition between bursting and beating. While irregular activity has been observed in the β-cell preparation (e.g., see Figs. 6–7 of reference 23), it has not been studied specifically. In this regard, we note that the conditions described above may be induced in the β-cell system by applying TEA and lowering temperature (I. Atwater, personal communication).

Convincing detection of deterministic chaos is facilitated if parameters can be controlled adequately and appropriate variables can be measured experimentally to identify (via systematic and slow parameter tuning) features of a known route to chaos such as period doubling. In some situations, the easily accessible variables are sufficiently revealing. In cardiac rhythm studies for example, recordings of membrane potential in the case of in vitro experiments (14) or arterial blood pressure for intact animals (18) have been useful. In our theoretical studies the voltage time courses of quite similar doublet patterns do not reflect visually the details of period-doubling.[2] In such a case recordings of the intracellular calcium level would be quite helpful. However, for some preparations, this experimental possibility awaits further technical development. When such recordings are available then one might even hope to generate an experimental one-variable map analogous to the theoretical ones computed here. We believe that for strongly calcium-dependent systems it is insightful to formulate simplified one-variable models in terms of calcium.

The mechanism for the oscillations explored here may be summarized roughly as follows. There is an underlying subsystem that exhibits some features of excitability and that has multiple steady and/or oscillatory states over a range of values for an identified parameter. This parameter is a dynamic variable (often acting on a slower time scale) for the full system that modulates the subsystem behavior. It exhibits net increase or decrease depending on which pseudo steady or oscillatory state of the subsystem is currently being expressed. When sufficient increases or decreases have accumulated, then activity switches to a different state because the current state of the subsystem has destabilized or disappeared (through coalescence with another state). This general interpretation may be applied in a variety of systems (19, 20, 22).[3] Consequently, such oscillatory systems may exhibit aperiodic behavior especially in parameter regions of transition behavior. Numerical simulations (not described here) of a bursting neuron model (24) also reveal aperiodic solutions. We remark that the models themselves need not be complicated; three variables are sufficient for continuous membrane models (25).

The aperiodic behavior that we report is inherent in the deterministic Chay-Keizer model. An experimental preparation or low-precision numerical calculation may be subject to detectable random noise. Hence, both deterministic and stochastic factors may contribute to observed aperiodicity. (We have verified the deterministic cause for the Chay-Keizer model by comparing our numerical results to

[2]To improve identifiability one might use plots (as described in reference 11) of $V(t + T)$ vs. $V(t)$ for T in some reasonable range and/or reliable interspike interval data.

[3]After this paper was submitted for publication the authors learned of a recent modeling study (Hindmarsh, J. L., and R. M. Rose. 1984. *Proc. Roy. Soc. Lond. B.* 221:87–102) of endogenous bursting in which aperiodic behavior was detected. The mathematical model, however, was not based upon a biophysical model as is the Chay-Keizer model.

those obtained with different integration schemes and error tolerances.) Studies of deterministic chaos have revealed parameter regimes with characteristic, and extremely fine-structured, interleaving regions for periodic and aperiodic behavior (e.g. see references 6, 11). The identification of predictable patterns, their parameter regions, and their order of appearance is a typical method by which one presents an argument for deterministic chaos. Dependent on the level of noise, one can expect many of these details to be obscured yet some features of a canonical route to chaos may be discernible just before the first appearance of aperiodicity. Indeed, Guevara et al. (14) identified various complex periodic patterns prior to observing chaos in the heart cell aggregate. The islet preparation however appears to be less tightly coupled (one typically finds near synchrony of burst patterns but not of individual spikes from cell to cell) so that the difference in properties between cells and the presence of noise may preclude distinguishing the two factors for aperiodicity, especially on the time scale of individual spikes. Perhaps a unicellular preparation or tightly-coupled islet might be better for quantitative comparisons between theory and experiment of periodic phenomena in endogenously bursting systems.

One may ask about the implications of aperiodic behavior from deterministic biological systems. In some cases, such as cardiac arythmias or neuronal epileptic activity, physiological pathologies may be direct functional consequences (26). In other cases functional meaning is less clear. If for the normally operating pancreas, islets are not synchronized with each other then periods of chaotic activity of individual islets may have little effect on pancreatic output. Nevertheless, for biophysical interpretation of experimental data on isolated islets or neurons one need not invoke hypotheses about environmental noise to account for observed aperiodic behavior. In many cases, such behavior can be quite consistent with, even supportive of, a simple deterministic model without stochastic elements.

This work was supported by a National Science Foundation grant PCM82 15583 to Dr. T. Chay.

Received for publication 23 April 1984 and in final form 2 October 1984.

REFERENCES

1. Atwater, I., C. M. Dawson, A. Scott, G. Eddlestone, and E. Rojas. 1980. The nature of the oscillatory behavior in electrical activity for pancreatic β-cell. *In* Biochemistry Biophysics of the Pancreatic-β-Cell. Georg Thieme Verlag, New York. 100–107.
2. Chay, T. R., and J. Keizer. 1983. Minimal model for membrane oscillations in the pancreatic β-cell. *Biophys. J.* 42:181–190.
3. Hodgkin, A. L., and A. F. Huxley. 1952. A quantitative description of membrane current and its application to conduction and excitation in nerve. *J. Physiol. (Lond.).* 117:500–544.
4. Fenstermacher, P. R., H. L. Swinney, and J. P. Gollub. 1979. Dynamical instabilities and the transition to chaotic Taylor vortex flow. *J. Fluid Mech.* 94:103–128.
5. Hudson, J. L., and J. C. Mankin. 1981. Chaos in the Belousov-Zhabotinskii reaction. *J. Chem. Phys.* 74:6171–6177.
6. Simoyi, R. H., A. Wolf, and H. L. Swinney. 1982. One-dimensional dynamics in a multicomponent chemical reaction. *Phys. Rev. Lett.* 49:245–248.
7. Testa, J., J. Perez, and C. Jeffries. 1982. Evidence for universal behavior of a driven nonlinear oscillator. *Phys. Rev. Lett.* 48:714–717.
8. May, R. H., and G. F. Oster. 1976. Bifurcations and dynamic complexity in simple ecological models. *Am. Nat.* 110:573–599.
9. Hofstadter, D. 1981. Metamagical themes. Strange attractors: mathematical patterns delicately poised between order and chaos. *Sci. Am.* 245:22–43.
10. Ott, E. 1981. Strange attractors and chaotic motions of dynamical systems. *Rev. Mod. Phys.* 53:655–671.
11. Swinney, H. L. 1983. Observations of order and chaos in nonlinear systems. *Physica.* 7D:3–15.
12. Wolf, A. 1983. Nonlinear dynamics: simplicity and universality in the transition to chaos. *Nature (Lond.).* 305:182–183.
13. Pomeau, Y., and P. Manneville. 1980. Intermittent transition to turbulence in dissipative dynamical systems. *Commun. Math. Phys.* 74:189–197.
14. Guevara, M. R., L. Glass, and A. Shrier. 1981. Phase locking, period-doubling bifurcations, and irregular dynamics in periodically stimulated cardiac cells. *Science (Wash. DC).* 214:1350–1353.
15. Hayashi, H., M. Nakao, and K. Hirakawa. 1982. Chaos in the self-sustained oscillation of an excitable biological membrane under sinusoidal stimulation. *Phys. Lett. A* 88:265–266.
16. Holden, A. V., and M. A. Muhamad. 1984. The identification of deterministic chaos in the activity of single neurons. *J. Electrophysiol. Tech.* 11:135–147.
17. Jansen, J. H., P. L. Christiansen, A. C. Scott, and O. Skovgarrd. 1983. Chaos in nerve. *Proc. IASTED (Intern. Assoc. Sci. Tech. Dev.) Symp., ACI.* 2:15/6–15/9.
18. Ritzenberg, A. L., D. R. Adam, and R. J. Cohen. 1984. Period multupling evidence for nonlinear behaviour of the canine heart. *Nature (Lond.).* 307:159–161.
19. Rinzel, J., and I. B. Schwartz. 1984. One-variable map prediction of Belousov-Zhabotinskii mixed mode oscillations. *J. Chem. Phys.* 80:5610–5615.
20. Rinzel, J., and W. C. Troy. 1983. A one-variable map analysis of bursting in the Belousov-Zhabotinskii reaction. *In* Nonlinear Partial Differential Equations. J. A. Smoller editor. American Mathematical Society, Providence. 411–428.
21. FitzHugh, R. 1960. Thresholds and plateaus in the Hodgkin-Huxley nerve equations. *J. Gen. Physiol.* 43:867–896.
22. Plant, R. E., and M. Kim. 1976. Mathematical description of a bursting pacemaker neuron by a modification of the Hodgkin-Huxley equations. *Biophys. J.* 16:227–244.
23. Meissner, H. P. 1976. Electrical characteristics of the beta-cells in pancreatic islets. *J. Physiol. (Paris).* 72:757–767.
24. Chay, T. R. 1984. Abnormal discharges and chaos in a neuronal model system. *Biol. Cybernetics.* 50:301–311.
25. Chay, T. R. 1985. Chaos in a three-variable model of an excitable cell. *Physica D.* In press.
26. Glass, L., and M. C. Mackey. 1979. Pathological conditions resulting from instabilities in physiological control systems. *Ann. NY Acad. Sci.* 316:214–235.